Journal of Molecular Graphics and Modelling 48 (2014) 1–8

Contents lists available at ScienceDirect

Journal of Molecular Graphics and Modelling

journal homepage: www.elsevier.com/locate/JMGM

Modeling the intermolecular interactions: Molecular structure of N-3-hydroxyphenyl-4-methoxybenzamide

Sedat Karabulut[a,*], Hilmi Namli[a], Raif Kurtaran[b], Leyla Tatar Yildirim[c], Jerzy Leszczynski[d]

[a] Balıkesir University, Faculty of Science and Literature, Department of Chemistry, 10145 Cagis, Balikesir, Turkey
[b] Akdeniz University, Alanya Faculty of Engineering, Materials Science and Engineering, Antalya, Turkey
[c] Hacettepe University, Department of Engineering Physics, Beytepe, 06800 Ankara, Turkey
[d] Jackson State University, Interdisciplinary Nanotoxicology Center, Jackson, MS, USA

ARTICLE INFO

Article history:
Accepted 16 November 2013
Available online 28 November 2013

Keywords:
Molecular structure
Dimer
Amide
X-ray
DFT

ABSTRACT

The title compound, N-3-hydroxyphenyl-4-methoxybenzamide (**3**) was prepared by the acylation reaction of 3-aminophenol (**1**) and 4-metoxybenzoylchloride (**2**) in THF and characterized by ^{1}H NMR, ^{13}C NMR and elemental analysis. Molecular structure of the crystal was determined by single crystal X-ray diffraction and DFT calculations. **3** crystallizes in monoclinic $P2_1/c$ space group. The influence of intermolecular interactions (dimerization and crystal packing) on molecular geometry has been evaluated by calculations performed for three different models; monomer (**3**), dimer (**4**) and dimer with added unit cell contacts (**5**). Molecular structure of **3**, **4** and **5** was optimized by applying B3LYP method with 6-31G+(d,p) basis set in gas phase and compared with X-ray crystallographic data including bond lengths, bond angles and selected dihedral angles. It has been concluded that although the crystal packing and dimerization have a minor effect on bond lengths and angles, however, these interactions are important for the dihedral angles and the rotational conformation of aromatic rings.

© 2013 Elsevier Inc. All rights reserved.

1. Introduction

The amide group always remains in the center of interest to scientists because of large variety of applications associated with compounds with such functional groups. Its presence in molecules may render them the property of efficient complexing agents, effective herbicides, in addition to importance of the amide fragment as the vital part of biomolecules [1].

The physical properties of —NH—CO— functional group have attracted attention of many experimental and theoretical scientists [2]. In addition to physical properties, also conformational properties of —NH—CO— group have been studied extensively. For example, formamide and substituted amides have been detected as planar species in both gas phase and solid state [3–9]. However, there are also some experimental results that report small deviations from planarity of amide functional group [6].

There are several applications of aromatic amide derivatives in crystal engineering [10] because of the very active participating properties (electron charge distribution, non-vanishing electrostatic multipole moment, magnetic ring current) of aromatic compounds in numerous interactions [11]. Nature of substituent generally affects the molecular geometry, reactivity, physicochemical and biological properties of aromatic compounds [12–14]. Based on the resonance or inductive effects of substituents they can be either classified as electron-donor or acceptor.

It is well known that hydrogen bonds are among interactions which are mostly responsible for arrangement of molecules in crystal structure [15]. Thus the molecular structures of aromatic amides should be well analyzed because of their diversity caused by hydrogen bonding capacity. Hydrogen bonding is one of the most important non-covalent interactions in the nature. The most famous examples of effects of hydrogen bonding on various species include property of water in different phases, structures and characteristics of proteins and nucleic acids [16].

The molecular geometry of a dimeric amide structure basically depends on three main factors; (i) the molecular properties of the molecule itself (stereochemical and stereoelectronic effects), (ii) effect of dimerization, (iii) crystal packing effects [17,18].

The title compound (Fig. 1) is an example of hydrogen bonded dimeric amide. As the result of a crystallization process millions of molecules are gather together into unique ordered arrangement. This arrangement is repeatable, under the same crystallization conditions [19].

In the present work experimental study has been complemented by computational approach. The geometric parameters of the title compound were calculated using following input

* Corresponding author. Tel.: +90 2666121000x1116; fax: +90 2666121215.
E-mail addresses: sedatk@balikesir.edu.tr, sedat@icnanotox.org (S. Karabulut).

1093-3263/$ – see front matter © 2013 Elsevier Inc. All rights reserved.
http://dx.doi.org/10.1016/j.jmgm.2013.11.001

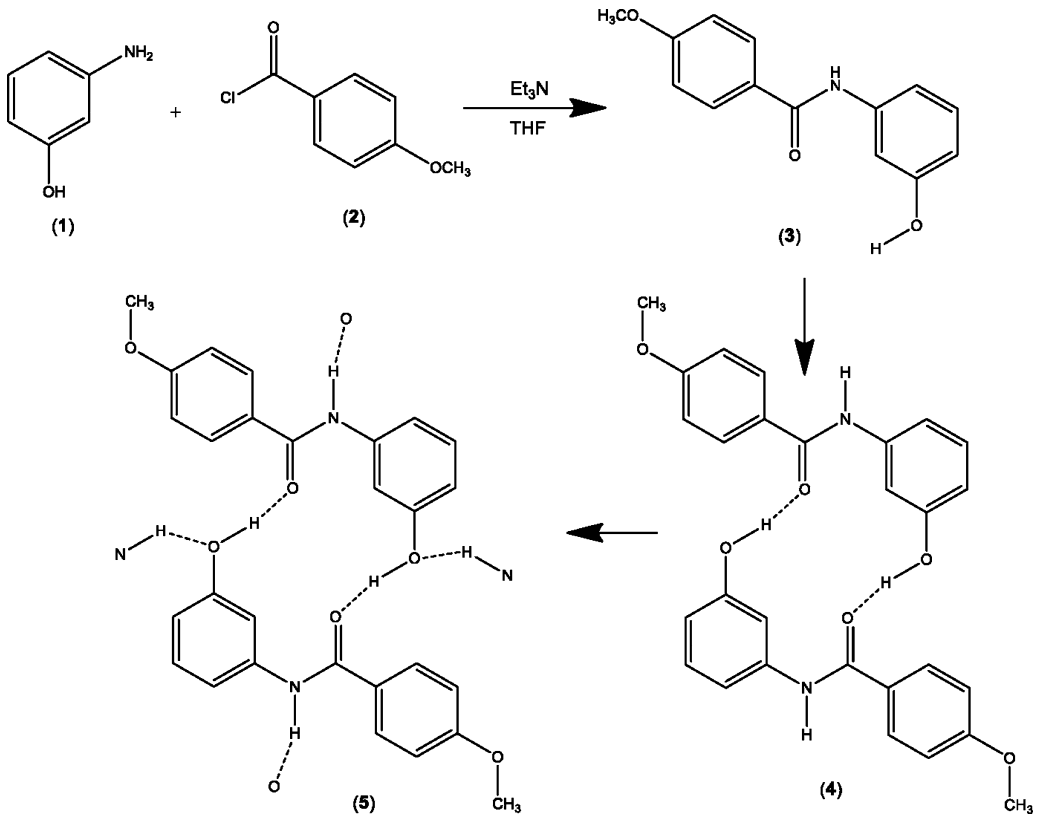

Fig. 1. Synthesis, dimerization and crystal packing of N-3-hydroxyphenyl-4-methoxybenzamide.

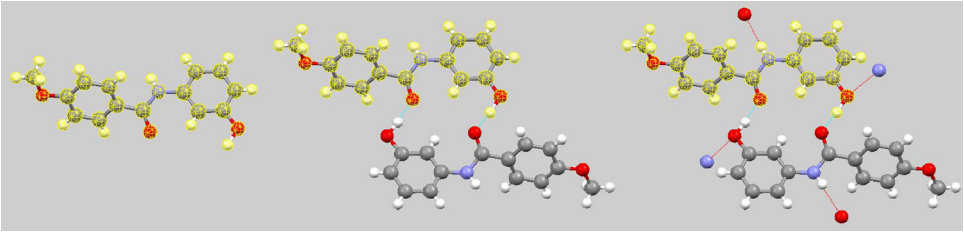

Fig. 2. Monomer (a), dimer (b) and dimer with unit cell contacts (c) input models. Highlighted parts were compared with the experimental X-ray results.

files: a monomer (**3**), a dimer (**4**), and a unit cell linked dimer (**5**). The monomer part of all optimized molecular geometries (Fig. 2) was compared with the analogous monomer part obtained from the X-ray crystallographic data. Bond lengths, bond angles and dihedral angles from experiment were compared with the predicted parameters. This comparison identifies the key driving force that governs the molecular geometry of N-3-hydroxyphenyl-4-methoxybenzamide monomer. The comparison of optimized monomer structure with experimental X-ray data provided the effect of internal dynamics of N-3-hydroxyphenyl-4-methoxybenzamide (substituents, stereochemical and stereoelectronic effects), the dimer structure calculation is for the investigation of the effect of dimerization on molecular geometry and the input file which has been constituted by definition of unit cell contacts is to understand the effect of crystal packing on molecular geometry. If dimerization and crystal packing are characteristic factors on the geometry of the title molecule, the regression between the calculated geometric parameters of **4** and **5** vs. experimental X-ray data should be better than **3**. The aim of this study was to make a complete theoretical and experimental structure analysis and identify the effective forces influencing the molecular geometry of title compound by using the experimental X-ray data as reference.

2. Materials and methods

2.1. Material

3-Aminophenol, 4-methoxybenzoylchloride, Et_3N, and THF were all purchased from Fluka and used without further purification.

2.2. Physical measurements

The elemental analyses were carried out at the Eurovector 3018 CHNS analyzer. The NMR measurements were carried out at the BRUKER DPX-400 FT-NMR Spectrometer. Perkin Elmer 1600 BX 2 FT-IR Spectrophotometer was used for FT-IR analysis.

2.3. Synthesis

N-3-hydroxyphenyl-4-methoxybenzamide was prepared according to the reported method [20]. 4-Methoxybenzoilchloride (2.7 ml, 0.02 mol) and 3-aminophenol (0.22 g, 0.02 mol) were dissolved and mixed in THF (30 ml). Three ethylamines (1.5 ml, 0.02 mol) were added dropwise to the mixture. The solution was stirred 15 h in ambient temperature and the white precipitate

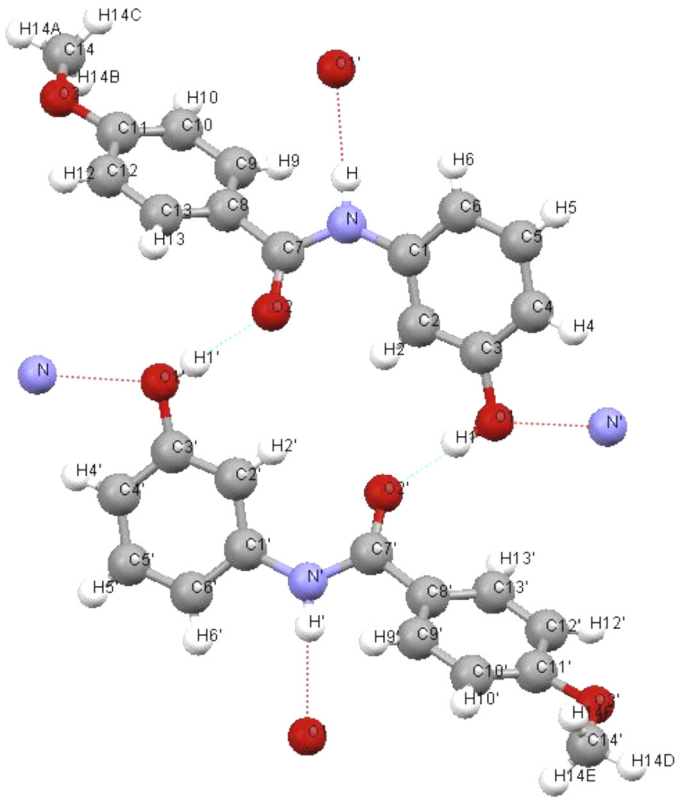

Fig. 3. Crystal structure of N-3-hydroxyphenyl-4-methoxybenzamide and labeling of atoms.

filtered. 70 ml water was added to the filtrate and the precipitate (product) filtered. The product was crystallized in the mixture of acetonitrile and methanol (5:1), m.p: 233–234 °C. ^{1}H NMR (DMSO) δ ppm: 7.3 (1H, s, H2); 9.3 (1H, e, H1); 6.5 (1H, d, H4); 7.1 (1H, t, H5); 7.2 (1H, d, H6); 9.9 (1H, e, H); 7.9 (2H, d, H9, H13); 6.9 (2H, d, H10, H12); 3.8 (3H, s, H14A, H14B, H14C) (Fig. 3). ^{13}C NMR (DMSO) δ ppm: 111 (C6), 108 (C5), 112 (C4), 132 (C3), 114 (C2), 130 (C1), 165 (C7), 162 (C8), 141 (C9, C13), 128 (C10, C12), 158 (C11), 55 (C14) (Fig. 3). Elemental analysis: %69.55 C, %5.69 H, %6.13 N.

2.4. Infrared spectrum

The FT-IR spectrum of reagents and the product was recorded at solid state with KBr pellet technique and overlaid for comparison (Fig. 4).

2.5. X-ray diffraction structure analysis

X-ray diffraction measurements were performed with CuK_α ($\lambda = 1.54184$ Å) radiation on an Enraf-Nonius CAD4 (κ-geometry) diffractometer, operating in $\omega/2\theta$ scan mode, equipped with a graphite-monochromated. The lattice parameters and their estimated standard deviations were determined from a least-squares refinement of 20 centered reflections in the range of $21.49° \leq \theta \leq 42.30°$ by using CAD4 Express [21]. During data collection, three standard reflections that were periodically measured every 120 min showed no significant intensity variation. A total of 4800 reflections were collected in the range $3.43° \leq \theta \leq 74.18°$, of which 4606 independent reflections were used for the structure determination. Data reduction was carried out using XCAD4 [22]. The structure was solved by direct methods and refined using the programs SHELXS97 and SHELXL97 [23], respectively, in the WinGX package [24]. A full-matrix least-squares refinement on F^2 converged at $R = 0.0642$. Atomic scattering factors were taken from the International Tables for X-ray Crystallography [25]. Hydrogen atoms of the OH and NH groups were taken from a difference Fourier map and fixed. The hydrogen atoms of phenyl and methyl groups were placed with $U_{iso}(H) = 1.2\,U_{eq}(C)$ and $U_{iso}(H) = 1.5\,U_{eq}(C)$, respectively. For all non-hydrogen atoms anisotropic displacement parameters were refined. Table 1 shows the crystal data and details of crystal refinement; Table 2 shows the atomic coordinates and equivalent isotropic displacement parameters. The ORTEP [26] drawing of the molecule is shown in Fig. 5. Hydrogen bond and molecular packing geometry of the title molecule were calculated with PLATON [27,28] and hydrogen bonding geometry is summarized in Table 3.

2.6. Computational details

Gaussian 03 [29] software was used for all calculations. Input files for monomer (**3**) and H-bonded dimer (**4**) was prepared based

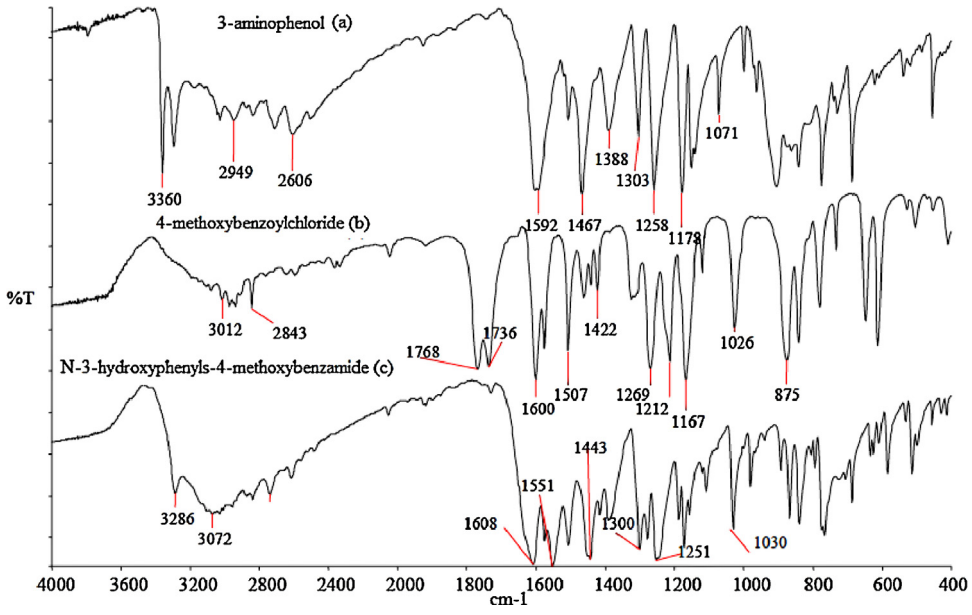

Fig. 4. The overlaid FT-IR spectra of the reagents (3-aminophenol and 4-methoxybenzoilchloride) and the product (N-3hydoxyphenyl-4-methoxybenzamide).

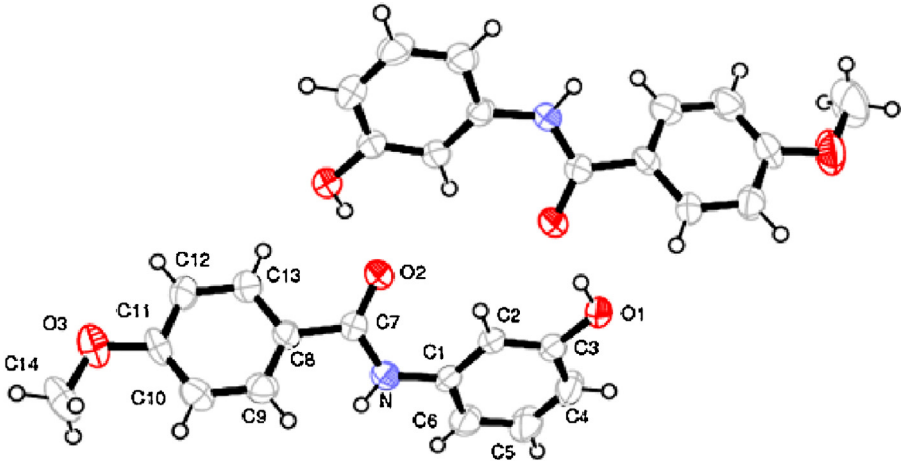

Fig. 5. ORTEP drawings of asymmetric units of N-3-hydroxyphenyl-4-methoxybenzamide.

Table 1
Crystal data and experimental details of the title compound.

Empirical formula	$C_{14}H_{13}NO_3$
Formula weight	243.25
Crystal system	Monoclinic
Space group	$P2_1/c$
Crystal shape/color	Prism/colorless
Volume (Å^3)	2422.8(15)
Z	8
D_{calc} (Mg/m^3)	1.334
Absorption coefficient (mm^{-1})	0.777
F(0 0 0)	1024
h, k, l ranges	$0 \rightarrow 16$, $-14 \rightarrow 0$, $-19 \rightarrow 19$
Refinement on F^2	$w = 1/[\sigma^2 F_0^2 + (0.1395P)^2]$, $P = (F_0^2 + 2F_c^2)/3$
Reflections collected/unique	4800/4606 [R_{int} = 0.0642]
Parameters	326
Goodness of fit on F^2	0.976
R indices [$I > 2\sigma(I)$]	R_1 = 0.0807, wR_2 = 0.1983
R indices [all data]	R_1 = 0.1831, wR_2 = 0.2562
Largest difference peak and hole (e/Å^3)	0.538 and −0.269

Additional material available from Cambridge Crystallographic Data Center as deposition numbers: CCDC 934952.

on experimental X-ray structure. However, the experimental data were modified for the unit cell linked structure (**5**), due to high computational expenses of the optimization of a complete crystal packing structure. In this modified input the HO— linkages were replaced by water and the HN— replaced by ammonia (Fig. 6). All structures were optimized at the B3LYP/6-31G+(d,p) [30,31] level. Vibrational frequency calculations have been performed after optimization and no imaginary frequencies were detected. Optimized results were compared with X-ray crystallographic data using bond lengths, bond angles, and selected dihedral angles which are responsible from the gauche conformation (Fig. 7) of aromatic rings.

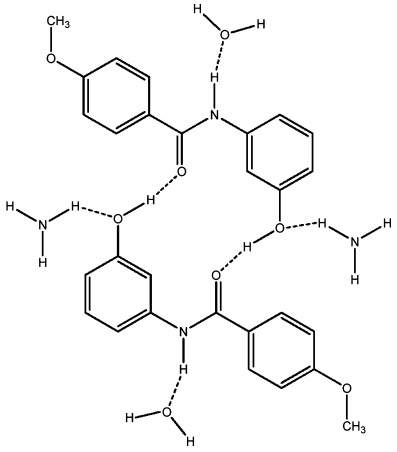

Fig. 6. Ammonia and water unit cell linkage model.

The input file of monomer has been generated by selecting the minimum energy geometry from three dimensional potential

Table 2
Atomic coordinates and equivalent isotropic displacement parameters for non-hydrogen atoms of two asymmetric units of the compound.

$$U_{eq} = \frac{1}{3}\sum_i \sum_j U_{ij} a_i^* a_j^* a_i a_j$$

Atom	x	y	z	U_{eq}(Å^2)
N	0.3808(3)	0.3566(3)	0.1877(2)	0.0479(9)
O1	0.02501(19)	0.2237(2)	0.13203(18)	0.0495(8)
O2	0.3936(2)	0.1764(3)	0.2351(2)	0.0620(9)
O3	0.8450(2)	0.3341(3)	0.4093(2)	0.0693(10)
C1	0.2778(3)	0.3550(3)	0.1389(3)	0.0398(10)
C2	0.2032(3)	0.2838(3)	0.1597(3)	0.0398(9)
C3	0.1025(3)	0.2892(3)	0.1112(3)	0.0418(10)
C4	0.0762(3)	0.3608(4)	0.0423(3)	0.0590(13)
C5	0.1512(4)	0.4314(4)	0.0224(3)	0.0675(15)
C6	0.2532(3)	0.4294(4)	0.0710(3)	0.0596(13)
C7	0.4327(3)	0.2715(4)	0.2335(3)	0.0441(10)
C8	0.5406(3)	0.2939(3)	0.2803(3)	0.0422(10)
C9	0.5696(3)	0.3941(4)	0.3240(3)	0.0484(10)
C10	0.6703(3)	0.4105(4)	0.3687(3)	0.0522(11)
C11	0.7424(3)	0.3288(4)	0.3685(3)	0.0480(11)
C12	0.7143(3)	0.2282(4)	0.3265(3)	0.0505(11)
C13	0.6142(3)	0.2092(4)	0.2832(3)	0.0483(11)
C14	0.8791(4)	0.4339(4)	0.4561(3)	0.0788(18)
N′	0.1110(2)	−0.1035(3)	0.3081(2)	0.0416(8)
O1′	0.4680(2)	0.0273(2)	0.35710(18)	0.0480(8)
O2′	0.0978(2)	0.0763(2)	0.2570(2)	0.0571(9)
O3′	−0.3506(2)	−0.0828(3)	0.0792(2)	0.0776(11)
C1′	0.2163(3)	−0.1023(3)	0.3537(2)	0.0367(9)
C2′	0.2905(3)	−0.0309(3)	0.3337(3)	0.0406(9)
C3′	0.3918(3)	−0.0402(3)	0.3776(2)	0.0399(9)
C4′	0.4199(3)	−0.1196(4)	0.4410(3)	0.0497(11)
C5′	0.3461(4)	−0.1909(4)	0.4602(3)	0.0530(12)
C6′	0.2440(3)	−0.1850(4)	0.4163(3)	0.0488(11)
C7′	0.0585(3)	−0.0186(4)	0.2620(3)	0.0431(10)
C8′	−0.0491(3)	−0.0423(3)	0.2154(3)	0.0413(10)
C9′	−0.0763(4)	−0.1420(4)	0.1723(3)	0.0528(11)
C10′	−0.1765(4)	−0.1610(4)	0.1250(3)	0.0579(13)
C11′	−0.2486(3)	−0.0784(4)	0.1235(3)	0.0511(12)
C12′	−0.2226(3)	0.0226(4)	0.1667(3)	0.0521(12)
C13′	−0.1227(3)	0.0417(4)	0.2122(3)	0.0464(11)
C14′	−0.3808(5)	−0.1814(5)	0.0300(4)	0.095(2)

Table 3
Details of hydrogen bonds between donor (D), acceptor (A) and hydrogen (H).

D—H···A	D—H (Å)	A···H (Å)	D···A (Å)	D—H···H (Å)
N—H···O1′[i]	0.86	2.17	3.026(5)	172
N′—H′···O1[ii]	0.87	2.14	3.004(4)	174
O1—H1···O2′[iii]	1.01	1.66	2.668(4)	175
O1′—H1′···O2[iv]	1.11	1.56	2.654(4)	167
C2—H2···O2	0.93	2.33	2.846(5)	114
C2′—H2′···O2′	0.93	2.33	2.874(5)	117

Symmetry codes [i = 1 − *x*, −1/2 + *y*, 1/2 − *z*; ii = −*x*, 1/2 + *y*, 1/2 − *z*; iii = *x*, −1 + *y*, *z*; iv = *x*, 1 + *y*, *z*].

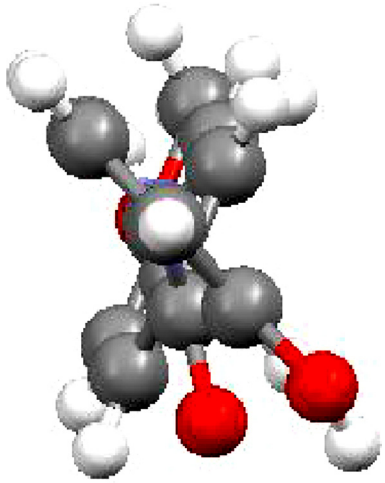

Fig. 7. Gauche conformation of two aromatic rings of N-3-hydroxyphenyl-4-methoxybenzamide.

energy surfaces (C_1—N, C_8—C_7 and energy) of the monomer which were calculated at semiempirical AM1 level [32].

Dimerization energy at B3LYP 6-31+G(d,p) level was calculated as 17 kcal/mol. Basis set superposition error has been considered at three basis sets levels (6-31+G(d,p), 6-311+G(d,p) and 6-311++G(2d,2p)). It has been concluded that there is no remarkable difference between the counterpoise corrections which has been calculated at different levels.

3. Results and discussion

There are two types of H-bonds in the crystal structure of the title compound: C=O···H—O and N—H···O—H (Fig. 3). Former are used for the dimerization and the latter connect the unit cells to build up the crystal structure. However, though the nitrogen electron lone pairs are better electron donor than the oxygen, they have no role in hydrogen bonding for this crystal packing system (Fig. 3). One of the main reason of this situation is the interaction of nitrogen lone pairs with carbonyl π* orbital. Fig. 8 shows the calculated HOMO of the title molecule. HOMO is generally located on one of the aromatic ring and nitrogen atom, due to the electron donating properties of —OH and —NH – and nitrogen lone pair electrons. As

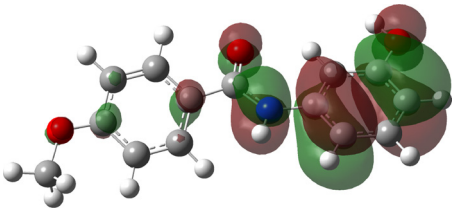

Fig. 8. HOMO of N-3-hydroxyphenyl-4-methoxybenzamide (isovalue = 0.02).

Table 4
The distance between the closest near X—H···π-ring surface.

X—H···π	H—π (Å)	C—π (Å)	X—H···π (°)
C5′—H5′···Cg1[a]	2.84	3.657(5)	147
C14—H14C···Cg2[b]	2.98	3.779(5)	141

Symmetry codes [a = 1 − *x*, 1 − *y*, 1 − *z*; b = 1 + *x*, 3/2 − *y*, 1/2 + *z*].

it can be seen from the orbital diagram (Fig. 8) lone pairs of nitrogen are delocalized to the carbonyl π* which explains why the lone pairs are not used to form intermolecular hydrogen bonds.

The crystal-packing have been structurally characterized by the single crystal X-ray crystallography. Single crystal X-ray diffraction analysis of prismatic-colorless crystal shows the crystallization in monoclinic system with space group $P2_1/c$. and cell constants are: $a = 13.167(3)$, $b = 11.880(3)$, $c = 15.830(8)$ Å, $\beta = 101.92(3)^\circ$.

X—H···Cg (π-ring) interactions were calculated using the PLATON software. Two closest near X—H···Cg interactions between asymmetric units have been identified. Planes of π-rings include Cg1: C8—C9—C10—C11—C12—C13 and Cg2: C8′—C9′—C10′—C11′—C12′—C13′, atoms, where the Cg refers to the ring center of gravity. [Cg1 = 0.64190(12), 0.31078(16), 0.32520(12), Cg2 = −0.14932(14), 0.94010(16), 0.16920(12)]. Details of the closest near X—H···π-ring interactions are given in Table 4.

The formation of amides by the reaction of amines and acylchlorides is a favorable reaction and the synthesis was completed without any heating of the reactants. The product has been successfully synthesized and purified by crystallization. The absence of the double absorption bands at 3360 cm^{-1} (symmetric and asymmetric stretching of amine functional group) and 1768 cm^{-1} (carbonyl stretching) at the spectrum of product (Fig. 4c) is one of the indications of the formation of amide functional group. The carbonyl stretching band at 1608 cm^{-1} represents another proof of successful synthesis. The results of NMR and elemental analysis are also consistent with the molecular structure of the obtained compound.

The hydrogen bond and covalent bond lengths of experimental X-ray structure have been compared with calculated bond lengths. The data displayed in Table 5 indicate that the hydrogen bonds of the dimer model (**4**) and unit cell contacted model (**5**) are almost identical, and both are shorter than the experimental results. Crystal structure effects may be suggested as one of the reasons for the difference between experimental and theoretical results.

Regression analysis has been carried out for calculated bond lengths and R^2 values obtained using the experimental X-ray bond lengths as a reference. R^2 values are 0.96, 0.97, 0.97 for monomer, dimer, and crystal pack optimized structures, respectively. Although R^2 values are similar, the sum of differences between experimental and calculated bond lengths ($\sum$ absolute (exp. bond length – calc. bond length)) has also been analyzed for a complete comparison (Table 6).

Interestingly, the sum of absolute bond length differences is quiet similar to the determined coefficients (R^2). Thus, it can be suggested that the dimerization and crystal packing have no significant effect on bond lengths of title molecule.

The effect of dimerization and crystal packing on the bond angles is similar to their effect on bond length when the distribution coefficients of bond angles are considered. The R^2 value is around

Table 5
Experimental and theoretical hydrogen bond distances.

	Experimental X-ray (Å)	Dimer (**4**) (Å)	Dimer with unit cell (**5**) (Å)
O2′···H1	1.81	1.75	1.73
O2···H1′	1.84	1.76	1.74

Table 6
Experimental (X-ray), theoretical (monomer, dimer, crystal pack) bond lengths (Å) and absolute differences between experimental and theoretical values.

Atom1	Atom2	Experimental X-ray	Theo. monomer	Theo. dimer	Theo. crystal pack	Absolute (Xray-mon.)	Absolute (Xray-dim.)	Absolute (Xray-cry. pack)
H1	O1	0.87	0.97	0.99	0.99	0.10	0.12	0.12
H	N	0.91	1.01	1.01	1.02	0.10	0.10	0.11
C2	H2	0.93	1.08	1.08	1.08	0.15	0.15	0.15
C9	H9	0.93	1.09	1.09	1.09	0.16	0.16	0.16
C13	H13	0.93	1.08	1.08	1.09	0.15	0.15	0.16
C10	H10	0.93	1.08	1.08	1.08	0.15	0.15	0.15
C4	H4	0.93	1.08	1.08	1.08	0.15	0.15	0.15
C6	H6	0.93	1.09	1.09	1.09	0.16	0.16	0.16
C5	H5	0.93	1.09	1.09	1.09	0.16	0.16	0.16
C12	H12	0.93	1.09	1.08	1.08	0.15	0.15	0.15
C14	H14A	0.96	1.10	1.10	1.10	0.14	0.14	0.14
C14	H14B	0.96	1.09	1.09	1.09	0.13	0.13	0.13
C14	H14C	0.96	1.10	1.10	1.10	0.14	0.14	0.14
O2	C7	1.25	1.23	1.24	1.24	0.01	0.00	0.00
N	C7	1.35	1.36	1.37	1.36	0.01	0.02	0.01
C3	C4	1.37	1.38	1.40	1.40	0.01	0.03	0.03
O3	C11	1.37	1.36	1.36	1.36	0.01	0.01	0.01
C11	C10	1.37	1.40	1.40	1.40	0.03	0.03	0.03
C4	C5	1.37	1.39	1.39	1.39	0.02	0.02	0.02
O1	C3	1.38	1.37	1.35	1.36	0.01	0.02	0.02
C12	C13	1.38	1.39	1.39	1.39	0.01	0.01	0.01
C2	C3	1.38	1.40	1.40	1.40	0.02	0.02	0.02
C12	C11	1.38	1.41	1.41	1.40	0.02	0.02	0.02
C1	C6	1.39	1.41	1.40	1.41	0.02	0.02	0.02
C8	C9	1.39	1.40	1.40	1.40	0.01	0.02	0.01
C9	C10	1.39	1.40	1.40	1.40	0.01	0.01	0.01
C2	C1	1.39	1.40	1.40	1.40	0.01	0.01	0.01
C6	C5	1.40	1.39	1.39	1.39	0.00	0.00	0.00
C8	C13	1.40	1.41	1.41	1.41	0.01	0.01	0.01
O3	C14	1.42	1.42	1.42	1.42	0.01	0.01	0.01
N	C1	1.42	1.41	1.42	1.42	0.01	0.00	0.00
C8	C7	1.48	1.50	1.50	1.50	0.02	0.02	0.02
Sum of absolute bond length differences						2.10	2.14	2.15

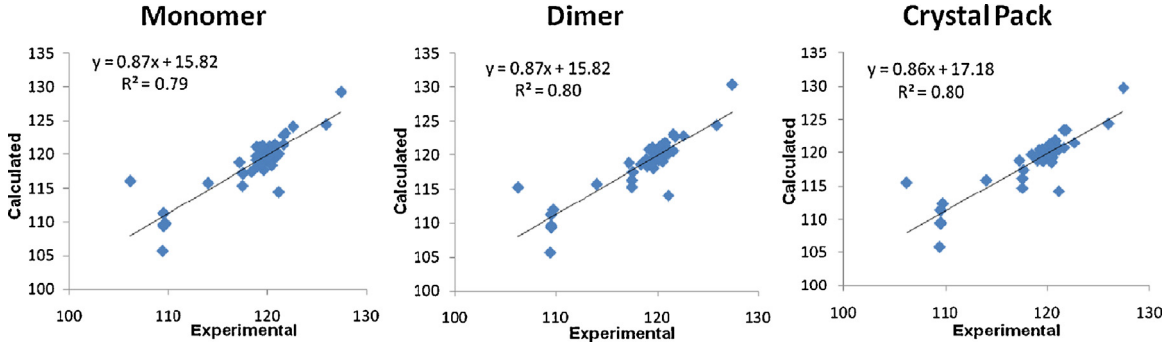

Fig. 9. Fitting graphics and determination coefficients of calculated bond angles for monomer (a), dimer (b) and crystal pack (c) models with experimental X-ray reference.

0.80 for all fitting graphics of bond angles (Fig. 9). As mentioned before there is another parameter to evaluate the consistency of calculated values – sum of absolute differences. The sum of absolute differences was computed as 65.6, 60.9 and 62.4 for monomer, dimer, and crystal packing models, respectively. When these values are taken into account, the dimer structure represents the closest model to the X-ray results. However, the differences among all predicted models are not significant. Therefore, it can be concluded that intermolecular interactions (dimerization and crystal packing) do not considerably effect on bond angles and bond lengths of the title molecule.

Some of the dihedral angles were not considered in the analysis because of fixed aromatic rings. However, rotatable dihedral angles were selected (Table 7) because of their remarkable effect on conformation. Selected experimental and theoretical dihedral angles were compared using the same methodology as described above. Though the R^2 values calculated are similar (Fig. 10), as those obtained in the bond length and angle comparison, however, the sum of calculated dihedral angles is considerably different (Table 7). As it can be deducted from the data in Table 7, dimerization and crystal packing especially affect two dihedrals (C13—C8—C7—N and C13—C8—C7—O2). These two dihedral angles characterize the position of methoxy substituted aromatic ring and amide functional

Table 7
Experimental and theoretical dihedral angles, sum of absolute differences of theoretical and experimental dihedral angles (Å).

	Experimental	Monomer model	Dimer model	Crystal pack model
C1—N—C7—C8	−179.5	−177.2	−176.9	−175.9
C1—N—C7—O2	2.5	3.5	3.8	4.1
C13—C8—C7—N	−142.0	−157.3	−150.0	−138.5
C13—C8—C7—O2	36.1	22.0	29.4	41.5
C14—O3—C11—C10	0.1	−0.2	0.5	1.6
H1—O1—C3—C4	168.7	179.7	179.0	178.8
Sum of absolute differences		43.9	29.3	25.7

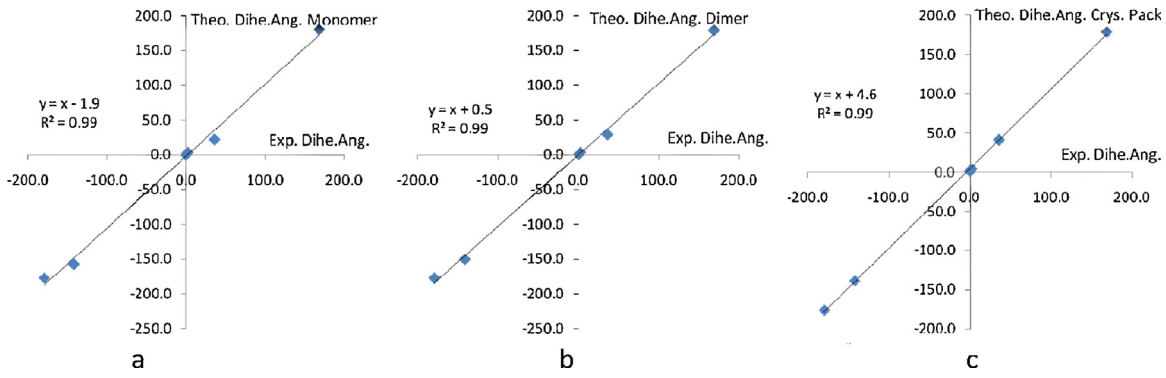

Fig. 10. Fitting graphics and determination coefficients of calculated dihedral angles for monomer (a), dimer (b) and crystal pack (c) models with experimental X-ray reference.

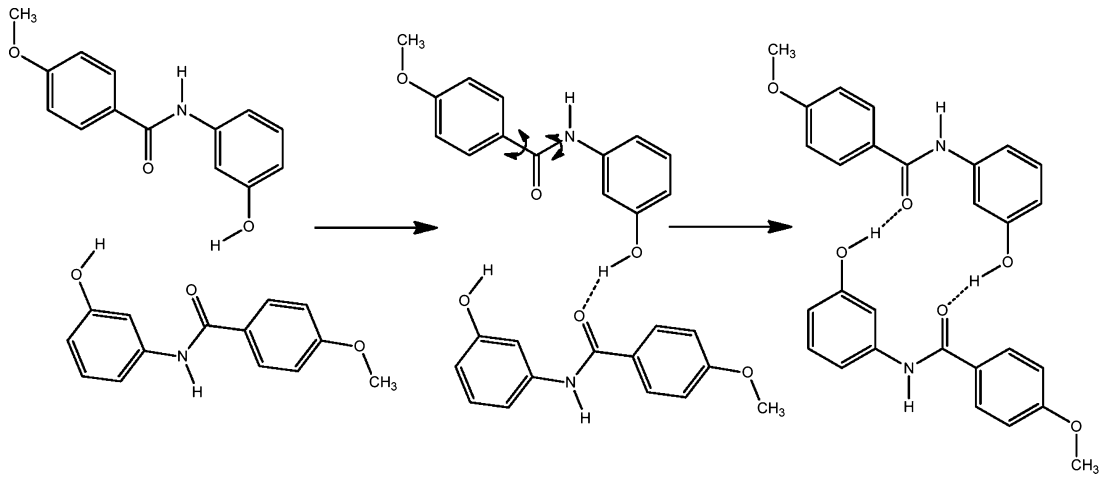

Fig. 11. Dimerisation steps of N-3-hydroxyphenyl-4-metoxybenzamide.

group. It is clear that the rotational preference of the C8—C7 bond is strongly affected by dimerization and crystallization.

This conclusion allows hypothesizing about the mechanism of crystallization of title molecule. Almost planar configuration (related to the arrangement of two aromatic ring and amide functional group) of the N-3-hydroxymethyl-4-methoxy benzamide monomer can be assumed. The first hydrogen bond is formed between H1 and O2. Then the C8—C7 bond rotates, to adopt the best position facilitating the formation of the second hydrogen bond (H1′—O2). Consequently, the dimer is formed (Fig. 11).

The binding energy has been calculated 17 kcal/mol and this energy may be supplied for the rotation of C8—C7 bond to connect monomers at best fitting geometry and build the crystal structure.

4. Conclusion

The goal of study is to explain the effect of various interactions governing molecular structure of title compound. The optimized monomer structure (**3**) represents the pristine, structural properties (stereochemical and stereoelectronical) of the compound. The dimer structure (**4**) additionally includes effect of dimerization. The last step, crystal packing optimization (**5**) covers also the effect of crystal packing. Obtained results showed that the bond lengths and bond angles are not affected by dimerisation and crystal packing. Contrary to bond angles and lengths, some of dihedral angles are highly depended on dimerization and crystal packing. From the obtained results it can be concluded that the studied kind of molecules form the crystal by arranging the dihedral angles to the most suitable position. Thus the crystal structures can be different from the monomer structures in solution, especially when dihedral angles are considered.

Acknowledgements

The authors acknowledge the Balikesir University, Hacettepe University and Jackson State University for the provided facilities for computational and experimental works.

References

[1] D. Kaur, P. Sharma, P.V. Bharatam, N. Dogra, J. Mol. Struct. (THEOCHEM) 759 (2006) 41–49.
[2] T. Kupka, I.P. Gerothanassisc, I.N. Demetropoulos, J. Mol. Struct. (THEOCHEM) 531 (2000) 143–157.
[3] E. Hirota, R. Sugisaki, R. Nielsen, C.J. Sorensen, J. Mol. Spectrosc. 49 (1974) 251–267.
[4] M. Kitano, K. Kuchitsu, Bull. Chem. Soc. Jpn. 47 (1974) 631–634.
[5] M. Kitano, K. Kuchitsu, Bull. Chem. Soc. Jpn. 46 (1973) 3048–3051.
[6] C.C. Costain, J.H. Dowling, J. Chem. Phys. 32 (1960) 158–165.
[7] M. Dreyfus, B. Maigret, A. Pullman, Theor. Chim. Acta 17 (1970) 109–119.
[8] E.D. Stevens, Acta Cryst. B 34 (1978) 544–551.
[9] H. Ohtaki, A. Funaki, B.M. Rode, G.J. Reibnegger, Bull. Chem. Soc. Jpn. 56 (1983) 2116–2121.
[10] S. Yamada, Y. Morimoto, Tetrahedron Lett. 47 (2006) 5557–5560.
[11] E. Mann, J. Mahıa, M.A. Maestrob, B. Herradon, J. Mol. Struct. 641 (2002) 101–107.
[12] M. Decouzon, O. Exner, J.F. Gal, P.C. Maria, J. Phys. Org. Chem. 7 (1994) 615–624.
[13] M. Schlosser, Angew. Chem. Int. Ed. Engl. 37 (1998) 1496–1513.
[14] K.V. Kilway, J.S. Siegel, Tetrahedron 57 (2001) 3615–3627.
[15] X. Gong, Z. Zhou, H. Zhang, S. Liu, J. Mol. Struct. (THEOCHEM) 718 (2005) 23–29.
[16] S.J. Grabowski, M. Palusiak, A.T. Dubis, A. Pfitzner, M. Zabel, J. Mol. Struct. 844–845 (2007) 173–180.
[17] C.F. Matta, C.C. Cow, S. Sun, J.F. Britten, P.H.M. Harrison, J. Mol. Struct. 523 (2000) 241–255.

[18] C.F. Matta, C.C. Cow, P.H.M. Harrison, J. Mol. Struct. 660 (2003) 81–97.
[19] J.F. Malone, C.M. Murray, M. Nieuwenhuyzen, G. Stewart, Chem. Mater. 9 (1997) 334–338.
[20] M. Mazik, D. Blaser, R. Boese, Tetrahedron 55 (1999) 12771–12782.
[21] Enraf-Nonius, CAD-4 Express Software. Version 1.1, Enraf-Nonius, Delft, Netherlands, 1993.
[22] K. Harms, S. Wocadlo, XCAD-4. Program for Processing CAD-4 Diffractometer Data, University of Marburg, Germany, 1995.
[23] G.M. Sheldrick, SHELXS97 and SHELXL97. Program for Crystal Structure Solution and Refinement, University of Göttingen, Germany, 1997.
[24] L.J. Farrugia, J. Appl. Cryst. 32 (1999) 837–838.
[25] A.J.C. Wilson, International Tables for Crystallography, vol. C, Kluwer Academic Publishers, Dordrecht, Netherlands, 1992.
[26] L.J. Farrugia, J. Appl. Cryst. 30 (1997) 565–566.
[27] A.L. Spek, PLATON2000, University of Utrecht, Netherlands, 2000.
[28] A.L. Spek, Acta Cryst. A46 (1990) C34.
[29] M.J. Frisch, G.W. Trucks, H.B. Schlegel, G.E. Scuseria, M.A. Robb, J.R. Cheeseman, J.A. Montgomery Jr., T. Vreven, K.N. Kudin, J.C. Burant, J.M. Millam, S.S. Iyengar, J. Tomasi, V. Barone, B. Mennucci, M. Cossi, G. Scalmani, N. Rega, G.A. Petersson, H. Nakatsuji, M. Hada, M. Ehara, K. Toyota, R. Fukuda, J. Hasegawa, M. Ishida, T. Nakajima, Y. Honda, O. Kitao, H. Nakai, M. Klene, X. Li, J.E. Knox, H.P. Hratchian, J.B. Cross, C. Adamo, J. Jaramillo, R. Gomperts, R.E. Stratmann, O. Yazyev, A.J. Austin, R. Cammi, C. Pomelli, J.W. Ochterski, P.Y. Ayala, K. Morokuma, G.A. Voth, P. Salvador, J.J. Dannenberg, V.G. Zakrzewski, S. Dapprich, A.D. Daniels, M.C. Strain, O. Farkas, D.K. Malick, A.D. Rabuck, K. Raghavachari, J.B. Foresman, J.V. Ortiz, Q. Cui, A.G. Baboul, S. Clifford, J. Cioslowski, B.B. Stefanov, G. Liu, A. Liashenko, P. Piskorz, I. Komaromi, R.L. Martin, D.J. Fox, T. Keith, M.A. Al-Laham, C.Y. Peng, A. Nanayakkara, M. Challacombe, P.M.W. Gill, B. Johnson, W. Chen, M.W. Wong, C. Gonzalez, J.A. Pople, Gaussian 03. Revision C. 02, Gaussian, Inc., Wallingford, CT, 2004.
[30] G. Parr, W. Yang, Density Functional Theory of Atoms and Molecules, Oxford University Press, New York, 1989.
[31] L.J. Bartolorri, K. Fluchick, Reviews in Computational Chemistry, vol. 7, VCH, New York, 1995.
[32] M.J.S. Dewar, E.G. Zoebisch, E.F. Healy, J.J.P. Stewart, J. Am. Chem. Soc. 107 (1985) 366–371.